ACS APPLIED MATERIALS & INTERFACES

Research Article

www.acsami.org

Effects of Block Length and Membrane Processing Conditions on the Morphology and Properties of Perfluorosulfonated Poly(arylene ether sulfone) Multiblock Copolymer Membranes for PEMFC

Luca Assumma,[†,‡] Huu-Dat Nguyen,[†,‡] Cristina Iojoiu,*[,†,‡] Sandrine Lyonnard,[⊥] Régis Mercier,[§] and Eliane Espuche[§]

[†]Univ. Grenoble Alpes, LEPMI, F-38000 Grenoble, France

[‡]CNRS, LEPMI, F-38000 Grenoble, France

[⊥]CEA-Grenoble, INAC/SPrAM, Groupe Polymères Conducteurs Ioniques, UMR-5819, CEA-CNRS-UJF, 17 Rue de Martyrs 38054 Grenoble, CEDEX 9 France

[§]Ingénierie des Matériaux Polymères, UMR-5223, IMP@LYON1, Université de Lyon, Université Lyon 1, 15 Bd. A Latarjet, 69622, Villeurbanne CEDEX France

Supporting Information

ABSTRACT: Perfluorosulfonated poly(arylene ether sulfone) multiblock copolymers have been shown to be promising as proton exchange membranes. The commonly used approach for preparation of the membrane is solvent casting; the properties of the resulting membranes are very dependent on the membrane processing conditions. In this paper, we study the effects of block length, selectivity of the solvent, and thermal treatment on the membrane properties such as morphology, water uptake, and ionic conductivity. DiMethyl-SulfOxide (DMSO), and DiMethylAcetamide (DMAc) were selected as casting solvents based on the Flory–Huggins parameter calculated by inversion gas chromatography (IGC). It was found that the solvent selectivity has a mild impact on the mean size of the ionic domains and the expansion upon swelling, while it dramatically affects the supramolecular ordering of the blocks. The membranes cast from DMSO exhibit more interconnected ionic clusters yielding higher conductivities and water uptake as compared to membranes cast from DMAc. A 10-fold increase in proton conductivity was achieved after thermal annealing of membranes at 150 °C, and the ionomers with longer block lengths show conductivities similar to Nafion at 80 °C and low relative humidity (30%).

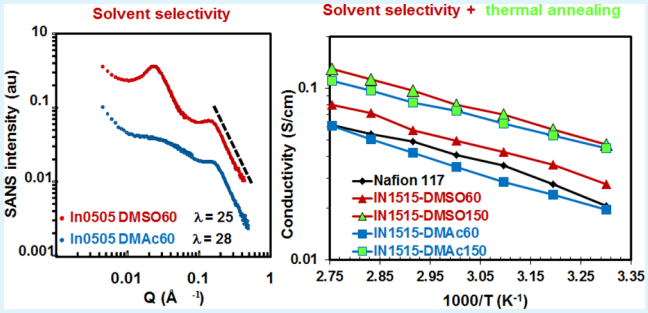

KEYWORDS: *perfluorosulfonated aromatic ionomers, block copolymer, polymer electrolyte membrane, PEMFC, solvent selectivity, membrane annealing*

1. INTRODUCTION

Proton exchange membrane fuel cells (PEMFC) are one of the most promising technologies to produce renewable energy. Among the components of PEMFC, the proton conducting membrane (PEM) plays a deciding role in system performances such as power density, durability, electricity cost, etc.[1] The membranes are, generally, based on ionomers. Among them, the most studied are the perfluorosulfonic acid ionomers (PFSA) such as Nafion or Aquivion because of their microstructure and high proton conductivity as well as superior chemical and electrochemical stabilities.[2−6] However, due to their high cost, low conductivities, poor mechanical strength, and high fuel permeability above 80 °C and at low relative humidity (RH), an alternative solution to Nafion and other PFSA membranes have to be found.[7−9] Therefore, a challenging issue lies in developing alternative PEMs toward low-cost and high-performance proton-conducting polymers with good mechanical properties and high conductivity at low RH.[10−12] The key success of advanced PEM is to design membranes with long-range continuity of both the conducting and the mechanically robust hydrophobic domains.[12−17] Therefore, ionomers able to self-organize attract a lot of attention for PEMFC application. Among them, the sulfonated aromatic multiblock copolymers were largely studied as PEM.[18−23]

As a result of the thermodynamic incompatibility among building blocks, the copolymers spontaneously self-organize, leading to phase separation and ordered nanostructures and hence providing materials with synergy of properties. Lee et al.[24] investigated the properties of PEMs consisting of

Received: March 3, 2015
Accepted: June 3, 2015
Published: June 3, 2015

DOI: 10.1021/acsami.5b01835
ACS Appl. Mater. Interfaces 2015, 7, 13808−13820

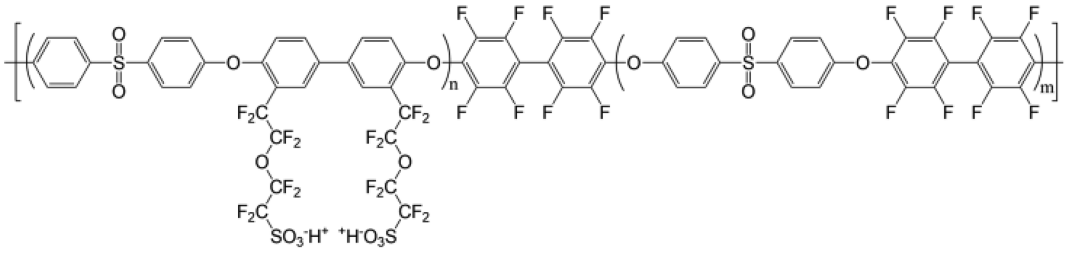

Ionomer: Inxx

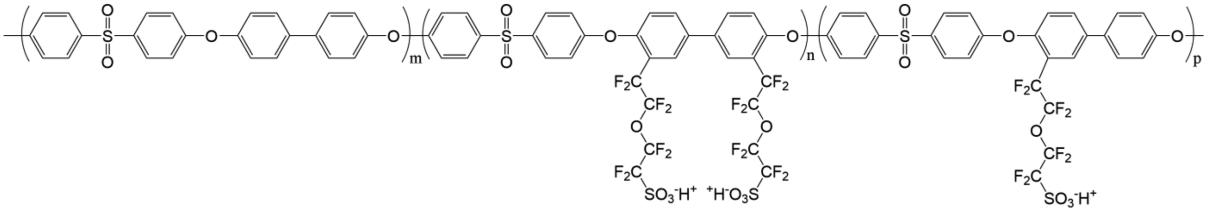

Radom Ionomer: ps-PES

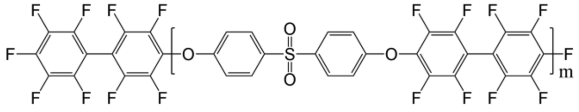

Hydrophobic block: FPES

Figure 1. Chemical structure of ionomers and hydrophobic block (FPES).

disulfonated and unsulfonated poly(arylene ether sulfone), and showed that the longer the blocks are, the higher the proton conductivity becomes. This effect was attributed to more continuously distributed hydrophilic domains.

Recently, another approach based on increasing the acidity of ionic functions was explored to enhance the proton conductivities of alternative PEMs. Aromatic ionomers bearing aryl sulfonimide acid[25,26] or alkyl perfluoro alkyl sulfonic acid side chains,[27−35] instead of aryl sulfonic acid, were considered. The poly(arylene ether)s bearing perfluorosulfonic acid side groups showed higher proton conductivity than poly(arylene ether)s functionalized with aryl sulfonic acid. In the spirit of sulfonated ionomers, further improvements of the proton-conducting properties were gained by designing block copolymer structures. Mikami et al.[35] and Assumma et al.[36,37] recently reported on perfluoroalkyl sulfonic acid-modified poly(arylene ether) and found that the bloc structure improves the proton-conductivities as compared to random ionomers with the same ion exchange capacity (IEC). Moreover, Assumma et al.[36,37] found that the partially fluorinated poly(arylene ether sulfone) multiblock copolymers bearing perfluorosulfonic functions lead to highly nanostructured membranes with morphology and conductivity close to those of Nafion.

In addition to the chemical structure and composition of ionomers, some pioneering works pointed out that the membrane preparing conditions are another critical factor to be considered for advanced PEM design.[38,39] Membranes are usually prepared by the casting method, i.e., dilute polymer solutions are cast onto a Petri Dish. The processing conditions drastically influence the microstructure[40] and the final properties of PEMs. In the case of block copolymers, the final morphologies of PEMs obtained by casting are strongly controlled by the interaction parameters between the casting solvent and each of the two blocks (A and B) ($\chi_{solv\text{-}A}$ and $\chi_{solv\text{-}B}$), as well as the interaction between blocks A and B ($\chi_{A\text{-}B}$).[41]

To evidence and understand the impact of processing conditions on PEM properties, some works were focused on the effects of casting solvent[24,42−47] and thermal annealing.[48−51] Recently, Lee et al.[24] reported on the high dependency between the proton conductivity of a block copolymer, the casting solvent nature, and the drying conditions.

The above considerations highlight that the design of new high performance ionomers requires to select molecular architectures capable of producing well-connected and efficient proton conduction pathways, on the one hand, and that significant optimizations can be reached, on the other hand, after adequately tuning the elaboration process conditions. In this work, we have investigated PEMs based on new poly(arylene ether sulfone) multiblock copolymers bearing perfluorosulfonic functions. We explored the potential of this class of ionomers by tuning the parameters, namely average block lengths and membrane processing conditions. The selected multiblock copolymers consist of fully perfluorosulfonated (ps-PES) and partially perfluorinated (FPES) polysulfones with three different lengths (for chemical structures, see Figure 1 and Table 1). A statistically random copolymer ps-PES with an ionic exchange capacity of 1.3 meq./g was also

Table 1. Average Blocks Molar Mass and IEC of Studied Block Copolymers and Random Ionomer

ionomers	ps-PES (g/mol)	FPES (g/mol)	IEC (meq H^+/g)
IN0505	5000	5000	1.30 ± 0.10
IN1010	10 000	10 000	1.35 ± 0.10
IN1515	15 000	15 000	1.32 ± 0.10
Ps-PES			1.30 ± 0.10

DOI: 10.1021/acsami.5b01835
ACS Appl. Mater. Interfaces 2015, 7, 13808−13820

considered as a control reference. We investigated the impact of casting solvent selectivity, block length, and annealing at 150 °C on the properties of interest, i.e., conductivity and water uptake. At the microscopic scale, the complex chemistry−selectivity interplay was scrutinized by measuring the phase-separated structural organization using small-angle neutron scattering. The conductivities of these ionomers are close to those of Nafion, while the mechanical properties are much better.[36] Moreover, these ionomers led, by casting in DMSO, to highly nanostructured membranes.[37] The detailed analysis of the structure-to-property relationship provided in this work can serve as guidelines for block copolymer optimization toward enhanced performances in fuel cells.

2. EXPERIMENTAL SECTION

2.1. Materials. Partially fluorinated poly(arylene ether sulfone) multiblock copolymers bearing perfluorosulfonic functions (Figure 1) were synthesized by regioselective bromination of partially fluorinated poly(arylene ether sulfone) multiblock copolymers (PES-FPES), followed by Ullman coupling reaction with lithium 1,1,2,2-tetrafluoro-2-(1,1,2,2-tetrafluoro-2-iodoethoxy)ethanesulfonate, as described previously.[36] The nomenclature for these copolymers is ionomer, Inxx, where x is the length of hydrophilic (ps-PES) and hydrophobic (FPES) blocks. For instance, In1010 refers to an ionomer with the length of segment ps-PES = 10 000 g/mol and of FPES = 10 000 g/mol. The ion-exchange capacity (IEC) has been determined by NMR and acid−base titration in organic solution and the protocols were described previously (Table 1).[36]

The random ionomer, ps-PES, with an IEC of 1.3 meq H^+/g was obtained by bromination of commercial polysulfone (Radel), followed by Ullman coupling reaction with lithium 1,1,2,2-tetrafluoro-2-(1,1,2,2-tetrafluoro-2-iodoethoxy)ethanesulfonate, as described previously (Figure 1).[36]

The FPES oligomer was synthesized by polycondensation of 4,4′-dihydroxydiphenylsulfone (DHDPS) with Decafluorobiphenyl (DFBP) purchased from Alfa Aesar, as described previously (Figure 1).[36]

2.2. Column Preparation and IGC Setup. In order to select the solvent for membrane casting, the interaction between the solvent and polymers were measured by inversion gas chromatography (IGC). The IGC experiments were performed using a PerkinElmer Clarus 480 gas chromatograph, equipped with a flame ionization detector (FID). The data acquisition was made with the AZUR software. High purity helium and methane were used as the carrier gas and marker, respectively. The flow rate of helium was measured with a soap bubble flowmeter connected at the end of the column, at room temperature. The experiments were performed at infinite dilution, by manually injecting 0.1 μL of each probe with a 1 μL Hamilton syringe. At least three injections of each probe were made, and the retention time was taken as the average of the three measurements. The retention times of the probes were determined by following the protocol described elsewhere.[52]

The following four solvents of the highest available purity (purchased from Aldrich), able to dissolve the Inxx copolymers, were used as probes: diMethylFormamide (DMF), diMethySulfOxide (DMSO), diMethyAcetamide (DMAc), and DiethyleneGlycoleDimetyhylEther (DGME) (Table 2). The stationary phase was prepared by coating the solid support, Chromosorb W HP (100/120) mesh (purchased by Antelia, France), with the polymer (ps-PES or FPES) by following the method proposed by Al-Saigh and Munkwas.[53] Acetone was used to prepare the polymer solutions of FPES and ps-PES in the lithium salt-form for coating. The process followed for the preparation of the column was described in detail elsewhere.[54,55] The IGC experimental conditions and the column characteristics are presented in Table 3.

Table 2. Physical Characteristics of Used Solvents for IGC

solvent	dipolar moment (μ)	dielectric constant (ε)	T_b (°C)
DMSO	3.9	47.3	189
DMAc	3.7	37.2	166
DMF	3.9	38.3	153
DGDE		7.3	140

Table 3. Chromatographic Conditions and Column Specifications

injector temperature (°C)	200
detector temperature (°C)	200
column temperatures (°C)	Ps-PES: 260, 265, 270, 275 FPES: 220, 230, 240, 250
column type of material	SS 316 ASTM A-269
column length (cm)	70
lumn O.D. (inch)	1/8
loading (%)	20.7
flow rate (mL/min)	10

2.3. Preparation of ps-PES and Inxx Membranes. The ionomers in the lithium salt form were dissolved in the two solvents that were chosen after calculation of the Flory−Huggins parameter from IGC analysis, i.e., DMSO and DMAc, respectively. The solution containing 7 wt % of Inxx in lithium salt form was stirred for 24 h at 60 °C. After that, the solution was centrifuged for 30 min at 5000 rpm to remove solid impurities. Then, the solution was degassed under vacuum for 30 min to remove the air bubbles. The degassed solution was cast onto a glass plate using a casting knife (Elcometer 4340 Automatic Film Applicator), and the solvent was evaporated in an oven at 60 °C.

In this work, we investigated the properties of "as-cast membranes" and "annealed membranes".

The "as-cast membranes" were obtained by following the protocol described by Assumma et al.[36] Then the membranes were rinsed many times in distilled water over 24 h to remove acid traces. The free solvent membrane was verified by ^{1}H NMR. The resulting block copolymer ionomer membranes in acidic form are named: $\text{Inxx}_{\text{solvent60}}$ (solvent DMAc or DMSO).

The annealed membranes are obtained from the "as-cast membranes". The "as-cast membranes" were submitted to an additional thermal treatment, i.e., after drying at 60 °C, they were annealed in a vacuum chamber at 150 °C for 24 h. The annealed membranes with a thickness ranging between 120 and 150 μm were then acidified following the same method than that use for the "as-cast membranes". The free solvent membrane was verified by ^{1}H NMR. The resulting block copolymer ionomer membranes in acidic form are named: $\text{Inxx}_{\text{solvent150}}$ (solvent DMAc or DMSO).

Nafion 117 membranes.

Nafion 117 membrane (thickness 176 μm) was reactivated before using.[36]

2.4. Water Uptake. The membranes Inxx or ps-PES in acidic form were vacuum-dried at 60 °C for 48 h, weighed, and immersed in deionized water at different temperatures ranging from 30 to 80 °C (the temperature was increased 10 °C each 24 h). The water uptakes (WU wt %) of membranes are reported in weight percent according to eq 1:

$$\text{WU} = \frac{W_{\text{wet}} - W_{\text{dry}}}{W_{\text{dry}}} \times 100 \quad (1)$$

where W_{wet} and W_{dry} are the weights of the wet and dry membranes, respectively.

The hydration number (λ), which is defined as the number of water molecules absorbed per sulfonic acid unit, was determined from the water uptake and the ion-exchange capacity (IEC) of the dry membrane, according to eq 2.

DOI: 10.1021/acsami.5b01835
ACS Appl. Mater. Interfaces 2015, 7, 13808−13820

Table 4. Values of Floy–Huggins Interaction Parameters Calculated from Net Retention Volume of the Probes Measured by IGC

T^a (°C)	$\chi^{\infty}_{FPES-DMAc}$	$\chi^{\infty}_{FPES-DMF}$	$\chi^{\infty}_{FPES-DGDE}$	$\chi^{\infty}_{FPES-DMSO}$	T^{**} (°C)	$\chi^{\infty}_{psPES-DMAc}$	$\chi^{\infty}_{psPES-DMF}$	$\chi^{\infty}_{psPES-DGDE}$	$\chi^{\infty}_{psPES-DMSO}$
220	0.34 ± 0.01	0.58 ± 0.03	0.65 ± 0.03	0.66 ± 0.03	260	−3.38 ± 0.1	−2.26 ± 0.1	−1.72 ± 0.1	
230	0.34 ± 0.01	0.55 ± 0.03	0.63 ± 0.03	0.65 ± 0.03	265	−3.19 ± 0.15	−2.18 ± 0.1	−1.66 ± 0.1	
240	0.34 ± 0.01	0.50 ± 0.03	0.73 ± 0.03	0.64 ± 0.03	270	−2.99 ± 0.1	−2.14 ± 0.1	−1.63 ± 0.1	−3.04 ± 0.16
250	0.31 ± 0.01	0.47 ± 0.02	0.77 ± 0.04	0.60 ± 0.03	275	−2.91 ± 0.1	−2.10 ± 0.1	−1.60 ± 0.1	−2.93 ± 0.15

$^a Tg_{FPES}$ = 220 °C, Td_{PES} = 530 °C; Tg_{psPES} =290 °C, and Td_{psPES} = 298 °C.

$$\lambda = \frac{WU \times 10}{IEC \times MW_{water}} \quad (2)$$

where MW_{water} is the molecular weight of water (18.01 g/mol).

2.5. Proton Conductivity. Proton conductivities of membranes at different temperatures and relative humidity (RH) were determined by measuring their resistances by impedance spectroscopy. The analysis is performed with Impedance analyzer Material Mates M2 7260 in the frequency range from 1 Hz to 10 MHz. The measurement of the membrane resistance is conducted through-plane with the help of the two in-lab made cells. The membrane is placed in-between the lower and the upper electrode (stainless steel), the pressure is applied by the spring on the upper electrode. In order to control the RH and the temperature, the measurements were carried out in a climatic chamber VC 4018 of Vötsch Industrietechnik. The measurements were performed at constant RH, i.e., 95% in the range of temperature from 30 to 90 °C or at constant temperature, i.e., 80 °C and 30–95% RH. The temperature (or RH) was increased with a step of 10 °C (10%), the measurements were performed after a stabilization time of 8 h.

2.6. Differential Scanning Calorimetry (DSC). The DSC measurements were performed using a DSC 1 STAR^e System from Mettler Toledo. The measurements were carried out under argon atmosphere with a heating scan of 20 °C per minute. The glass transition temperatures of "as-cast" and "annealed membrane" were determined from the first heating scan performed from 25 to 300 °C.

2.7. Small Angle Neutron Scattering (SANS). SANS measurements were performed on the D22 spectrometer at the Institut Laue Langevin, Grenoble, France. The measurement protocol, briefly presented here, is similar to that we described in ref 36. Thus, two configurations were used to cover an extended Q-range from 8.5 × 10^{-3} to 0.6 Å^{-1}, Q being the scattering vector defined as $Q = (4\pi/\lambda)\sin(\theta/2)$ where λ is the wavelength of the incident neutron beam, and θ is the total scattering angle. The isotropic 2D patterns recorded in the two configurations were radially averaged to obtain the 1D scattered intensities $I(Q)$, and further corrected using standard procedures (detector efficiency, background, and empty cell subtraction). As data taken in the two configurations were perfectly overlapping in the intermediate Q-region, the $I(Q)$ were merged to obtain a single spectrum for each sample. Prior to the SANS experiment, the membranes were inserted in quartz Helma cells, closed quickly, and maintained at room temperature.

2.8. NMR Spectroscopy: Residual Solvent Analysis. ^{1}H NMR spectroscopy was conducted on a Bruker Avance 400 spectrometer. For membranes prepared from DMAc, a 0.07-g portion of membranes was dissolved 0.7 mL in DMSO.d6 and NMR spectra was obtained after 64 scans. For membranes cast from DMSO, the membrane was dissolved DMF.d7.

Chemical shift of membranes cast from DMAc:

^{1}H NMR: (DMSO.d6): The peaks at δ (ppm) 7.90–8.20 (m), 7.48 (d), 7.34–7.18 (m) were attributed to the aromatic protons of ionomer Inxx and the peaks at δ (ppm) 2.946 (s), 2.787 (s), 1.961 (s) for DMAc.

Chemical shift of membranes cast from DMSO:

^{1}H NMR: (DMF.d7): The peaks at δ (ppm) 8.45–8.25 (m), 7.8 (d), 7.65–7.45 (m) f were attributed to the aromatic protons of ionomer Inxx and the peaks at δ (ppm) 2.478 (s) for DMSO.

The amount of DMAc residual solvents (wt %) or solvent contain (SU) and the solvation number (λ_{sol}), which can be defined as the number of solvent molecules absorbed per ionic function, in the ionomer films for the "as-cast membranes" and "as-annealed membranes" was calculated with eqs 3 and 4:

$$\lambda_{sol} = \frac{[solvent]}{[SO_3H]} = \left(\frac{I_{sol}}{N_{sol}}\right) \Big/ \left(N_{Ion} \times \frac{I_{pol}}{N_{pol}}\right) \quad (3)$$

$$SU = \frac{\lambda_{sol} \times IEC \times MW_{solvent}}{10} \quad (4)$$

where I_{sol} is the integral of solvent peak, I_{pol} is the integral of ionomer peak region (from 7.1 to 8.3 ppm for DMSO.d6 and from 7.3 to 8.5 ppm for DMF.d7), N_{sol} is the number of hydrogen corresponding to each solvent peak (N_{sol} = 3 for DMAc and 6 for DMSO), N_{ion} is the number of ionic unit per polymer repeating unit (N_{ion} = 2), N_{pol} is the number of hydrogen per polymer repeating unit corresponding to polymer peak (N_{pol} = 27.32), IEC is the ionic-exchange capacity (meqH^+/g), and $MW_{solvent}$ is the momecular weight of the solvent (DMAc 87.12 g/mol and DMSO 78.13 g/mol).

2.9. Gas Permeability. The permeation experiments were performed under an anhydrous state for hydrogen and oxygen. The membrane was placed between the two compartments of the permeation cell. The effective membrane area was 3 cm^2. The cell was thermostated at 20 ± 1 °C. A preliminary high vacuum desorption was realized to ensure that the static vacuum pressure changes in the downstream compartment were smaller than the pressure changes due to the gas diffusion. A 3.0 × 10^5 Pa gas pressure was introduced in the upstream. The evolution of the pressure in the downstream compartment was followed with a datametrics pressure sensor. A steady-state line was obtained after a transitory state by plotting the measured pressure versus time. The permeability coefficient, P, expressed in barrer unit (1 barrer = 10^{-10}cm$^3_{STP}$ cm cm^{-2} s^{-1} cm$_{Hg}^{-1}$ = 7.5 × 10^{-18}Nm^3·m·m^{-2}·s^{-1}·Pa^{-1}= 3.348 × 10^{-16} mol·m·m^{-2}·s^{-1}·Pa^{-1}), was calculated from the slope of the steady-state line.

2.10. Dynamic Mechanical Analysis (DMA). DMA was performed with DMA Q800 device of TA Instruments in the temperature range from 20 to 350 °C using a temperature ramp of 2 °C·min^{-1}. Data treatment was performed with TA Universal Analysis software. The dried membranes, in lithium form, of average dimensions 15 × 6 mm^2 and thickness of 120–160 μm are introduced in the clamp of film tension. The following settings are chosen: multifrequency-strain mode, frequency 1.0 Hz, preload force 0.1 N, force track 150%, and strain deformation was fixed at 0.05%.

3. RESULTS AND DISCUSSION

3.1. Solvent Selectivity. The degrees of solvent selectivity of casting solvents for the component blocks were determined by measuring the Flory–Huggins parameter of ps-PES and FPES by IGC. The Flory–Huggins theory allows the calculation of the polymer–solvent interaction parameter (χ^{∞}_{p-s}). This parameter is considered as a crucial criterion to select a suitable solvent for an industrial process and also to predict solubility, degree of swelling, or polymer–solvent compatibility.

By IGC technique, the material under study (ps-PES and FPES) is packed into the column into which carefully selected probes, i.e., solvents (Tables 2 and 4) were injected at infinite

DOI: 10.1021/acsami.5b01835
ACS Appl. Mater. Interfaces 2015, 7, 13808–13820

dilution concentration in order to make sure that the retention is governed by the stationary phase (ps-PES, FPES) and -probe (solvent) interactions as well as the probe−probe interactions are avoided.[55] The key measurement in IGC experiments is the net retention volume of the probes, V_N that it is expressed as the volume of the carrier gas necessary to elute the solute from the column and allows one to calculate the Flory−Huggins interaction parameter χ^{∞}_{p-s} [56] (see Supporting Information, SI) (Table 4). According to the Flory−Huggins theory, values of the interaction parameter smaller than 0.5 are indicative of good solvents for the material under study, whereas values greater than 0.5 represent an unfavorable polymer−solvent interactions.[55] On the basis of this statement from Table 4, it can be concluded that only DMAc is a good solvent out of the four employed solvents for FPES segment. Concerning the interaction parameters for the segment ps-PES, all the $\chi^{\infty}_{ps-PES-S}$ values are negative, and the lowest values are obtained with DMSO followed by DMAc. However, the measurements of V_N for the ps-PES were performed at a temperature lower than its Tg in order to avoid the degradation of ps-PES (Tg and Td are very close, 290 and 298, respectively[36]). Thus, the χ^{∞}_{p-s} calculated in this case is more representative of the interactions between the solvent and the surface of ps-PES coated silica. However, the calculated values of χ generally decrease with an increase in the temperature. This is attributed to enhanced segmental motions of polymer chains at higher temperatures, thus creating an extra free volume with which the probe can interact.[56] Therefore, if the measurements were performed at higher temperature, then even lower values could be obtained. However, in order to confirm that DMSO and DMAc are good solvents, we also performed a solubility test for ps-PES. We observed that more than 50 wt % of ps-PES was dissolved in both solvents at room temperature. These results fully corroborate the observation that DMSO and DMAc are good solvents for ps-PES.

On the basis of these results, we selected to work with (i) DMAc as the casting solvent which is able to dissolve both blocks of ionomers Inxx and (ii) DMSO as a selective solvent able to dissolve the ionomers Inxx but being a good solvent only for ps-PES block.

3.2. Morphology of PEMs. A morphological study was conducted using SANS to investigate the effect of solvent selectivity on the resulting microstructure of multiblocks copolymers films. In Figure 2, we display the SANS profiles of hydrated ps-PES and block copolymers cast at 60 °C in DMSO and DMAc, prepared at intermediate hydration numbers (λ in the range 25−29). For ps-PES (Figure 2a), we observe a well-defined and intense scattering maximum in the Q-range, where the ionomer peak is usually observed in PFSA materials ($Q \approx 0.13$ Å^{-1}). The ionomer peak is the signature of hydrophilic/hydrophobic phase separation at the nanoscale. The ps-PES polymers therefore exhibit nanoscale organization with mean separation distances between ionic domains, $d_{ionic} = 2\pi/Q_0$, where Q_0 is the position of the ionomer peak, equal to 5 nm at hydrations $\lambda \approx 25$. As the shape and position of the ionomer peaks for ps-PES cast in DMSO and DMAc are similar at the same local hydration, we can conclude that the casting solvent does not significantly impact the ionic nanodomain organization in ps-PES ionomers. The SANS profiles of the cast block copolymer In0505 (Figure 2b) were measured on a more extended Q-range and are compared in Figure 2b. The block copolymer membrane SANS spectra exhibit two prominent features: an ionomer peak located typically at $Q \approx 0.15-0.2$ Å^{-1}, as in the ps-PES, and an additional low-angle scattering intensity at $Q \approx 0.02-0.03$ Å^{-1}, which can be ascribed to structural correlations between hydrophobic block domains.

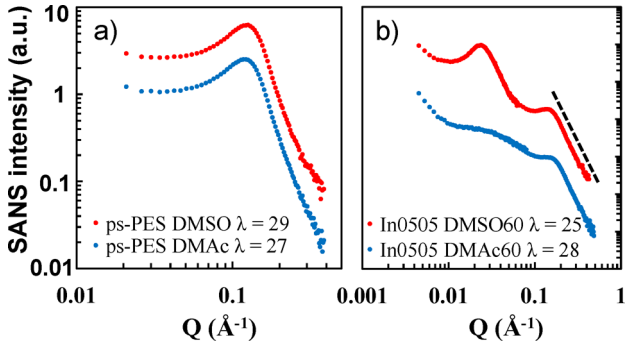

Figure 2. SANS profiles of ps-PES (a) and In0505 (b). The spectra have been shifted for clarity. The ionomer peak at $Q \approx 0.1-0.2$ Å^{-1} is the signature of nanophase separation between ionic domains and polymer backbone. An additional low-Q peak is found in block copolymer membranes, as due to the self-organization of hydrophilic/hydrophobic blocks.

The presence of two scattering maxima indicates a complex multiphase polymer organization at typical length scales of few nanometers and few tens of nanometers. These characteristic features are impacted by the choice of the casting solvent. The well-defined high-Q ionomer peak is found in the same Q-range for $IN0505_{DMSO60}$, $IN0505_{DMAc60}$, and ps-PES ionomers. We observe some broadening of the peak in the DMAc-cast membrane, which can indicate a more disordered distribution of ionic domains than in DMSO-cast and ps-PES membranes. Yet, in these materials, the formation of ionic domains appears to be rather insensitive to the block architecture and the casting solvent. Therefore, it is predominantly triggered by the common presence of perfluorinated pendent chains bearing acidic functions. In contrast, the low-Q correlation feature appears to be drastically affected by the nature of the solvent. The peak is very intense and sharp in DMSO-cast block copolymers, while a large and ill-defined correlation bump is observed in DMAc-cast membranes. Note that such a low-Q feature does not exist in ps-PES polymers, as the low-angle scattering is flat—although not measured at the same low Q values as In0505. Hence, we can conclude that the film cast in DMSO presents a remarkable structural organization due to the self-assembly of blocks units forming large-scale ordered domains,[37] while block segregation is not favored when using DMAc as a solvent, such that a more random distribution of hydrophobic and hydrophilic segments leads to poor long-range order. This behavior can be consistently rationalized in terms of solvent affinity with the blocks. The DMSO film casting process produces enhanced long-range order due to the selectivity of DMSO (as described in section 3.1) relatively to DMAc. FPES chain segregation is favored by (i) the low solubility of FPES in DMSO solvent and (ii) the immiscibility between ps-PES and FPES blocks. These effects contribute to the formation of well-structured FPES domains at high ionomer dilution. Contrarily, DMAc being a good solvent for both blocks, it plays the role of compatibilizer. Because of their intrinsic chemical incompatibility, the two blocks tend to separate at high polymer concentration, and a drastic decrease in copolymer chain mobility yields to the formation of more disordered hydrophobic domains.

DOI: 10.1021/acsami.5b01835
ACS Appl. Mater. Interfaces 2015, 7, 13808−13820

These findings suggest that the casting solvent significantly affects the large-scale blocks organization, with a limited effect on nanoscale phase separation between ion-containing domains and polymer backbone. The choice of a casting solvent able to compatibilize the blocks introduces structural disorder into the multiscale morphology. Further insights into the ionic domain organization can be gained by inspecting the swelling behavior of the cast membranes. Ionomer films were prepared over an extended range of hydration numbers, from λ = 0 to 46 mol water/mol SO_3H, to evaluate in detail the membrane structure at the nanoscale. In Figure 3, we display the incoherent background-subtracted SANS spectra of swollen membranes cast in DMAc (a) and DMSO (b) for In0505.

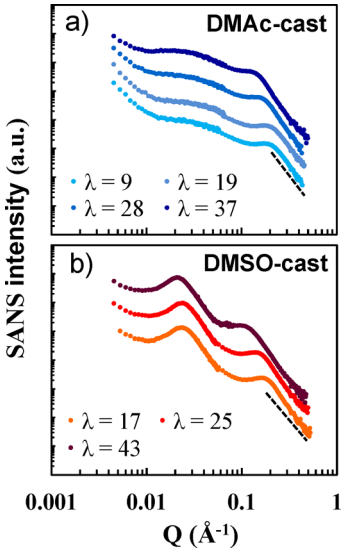

Figure 3. Evolution of SANS spectra of the aromatic ionomers upon water content. λ is the number of water molecules per ionic group. (a) $In0505_{DMAc60}$ and (b) $In0505_{DMSO60}$. The spectra are shifted in intensity for clarity. The dashed lines represent the Q^{-4} Porod behavior, indicating the presence of a sharp interface at the nanoscale.

The ionomer peak present in both films increases in intensity and shifts toward smaller Q values as the hydration is increased, evidencing the continuous increase of d_{ionic} correlation distances due to nanoscale swelling. The incorporation of water molecules within the hydrophilic phase significantly increases the volume of the hydrophilic domains (therefore raising the correlation distance) while enhancing the SANS contrast. The same behavior characterizes also the low-Q peak (hydrophobic peak), showing that the block domains are moved apart along hydration. Interestingly, we note that the low-Q peak of DMAc-cast membranes remains larger and less pronounced as compared with that of DMSO cast films over the whole hydration range.

The nanoscale swelling can be quantitatively analyzed by extracting the characteristic correlation distances d_{ionic} from the ionomer peak positions and plotting the dilution law $d_{ionic} = f(\lambda)$. As seen in Figure 4a, d_{ionic} expands from 3 to 6 nm typically, with similar variations for both films (DMSO and DMAc) as a function of λ. Furthermore, the expansion of ionic domains $d_{ionic} - d_0$ can be extracted, d_0 being the λ = 0 interpolation of the swelling law (Figure 4b). The obtained linear behavior with a slope close to 1 is comparable to that of Nafion membrane. Such behavior can be ascribed to the dilution of a locally two-dimensional structure and was

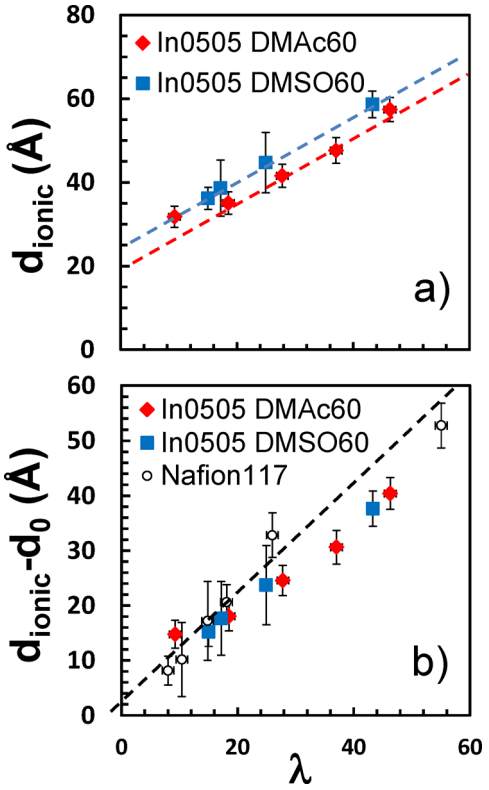

Figure 4. (a) Swelling law, i.e., mean separation distances between ionic domains, d_{ionic}, as a function of the hydration number λ. (b) Ionic domains mean size, $d_{ionic} - d_0$, as a function of the hydration number. The d_0 values are extrapolated from the swelling law at λ = 0.

interpreted for PFSA materials in the framework of a semilamellar local morphology[57,58] or ribbon-like hydrophobic aggregates.[59]

Clearly, the nanoscale swelling of ionic domains in DMSO and DMAc cast membranes is due to the selective incorporation of water in the highly hydrophilic sulfonate-containing regions. This is mostly driven by the nature of local interactions between charged species and the low water wettability of hydrophobic pendant chain, independently from the chemical architecture of ps-PES and FPES main chains and their self-assembling behavior.

Complementary information on the hydrophobic/hydrophilic phase separation can be gained by extracting the area of polymer−water interface per polar head (specific surface) from the asymptotic behavior of the scattering curves at large Q-values (Figure 5). In the presence of a sharp polymer−water interface, the intensity has to scale as Q^{-4} according to the Porod's law. The specific surface σ can be extracted from eq 5:

$$\lim_{q\to\infty} \frac{Iq^4}{\Phi_p} = 2\pi\Delta\rho^2\Phi_p\frac{\sigma}{\nu_0} \qquad (5)$$

where $\Delta\rho$ is the scattering length density difference between the hydrophobic block and the hydrophilic block, while ν_0 is the average volume of polymer per repeat unit of hydrophobic block. As we need to compare the same polymer cast with different solvents, the impact of solvent can be evaluated by considering the ratio of the high-Q intensities for the film cast in DMAc/DMSO (eq 6).

DOI: 10.1021/acsami.5b01835
ACS Appl. Mater. Interfaces 2015, 7, 13808−13820

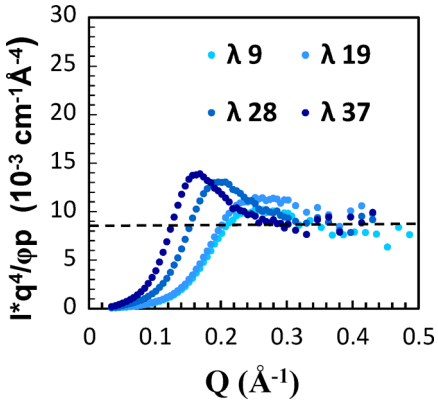

Figure 5. Porod representation of SANS spectra for $In0505_{DMAc60}$. The dashed line represents the high-Q asymptotic plateau showing the presence of a sharp interface.

$$\frac{\left(\frac{IQ4}{\phi p}\right)DMAc}{\left(\frac{IQ4}{\phi p}\right)DMSO} = \frac{\sigma DMAc}{\sigma DMSO} \quad (6)$$

Then, the experimental value of the ratio directly informs on the nature of the interface. A value of 1.3 is found that corresponds to an increase of specific surface in DMAc-cast films by 30% as compared to that obtained in DMSO. The higher specific surface for the DMAc-cast membrane is consistent with the ill-defined large-scale organization due to unfavored block segregation, as previously discussed. A more randomly distributed ill-defined block structure indeed implies that the hydrophilic domains are likely to be more isolated and less connected as compared to the film cast in DMSO. This observation points out that the membrane morphology is determined by the local topology of ionic domains, which similarly expands upon hydration in DMSO or DMAc cast membranes, as well as the ionic network connectivity (better in DMSO-cast membranes). Both properties are likely to impact the performance in terms of water uptake and conductivity, as will be investigated in detail in the following sections.

3.3. Thermo-Mechanical Properties. The impact of casting solvent on the thermo-mechanical properties of membranes In0505 were investigated by measuring the temperature dependent storage modulus and tan δ spectra (Figure 6a–c) by DMA. The measurements were performed on membranes based on ionomers in lithiated form in order to avoid the ionomer degradation at temperatures higher than 200 °C.[36] The thermo-mechanical response of the membranes is shown to significantly differ depending on the elaboration solvent. Indeed, the storage modulus of the membrane cast in DMSO shows two relaxation temperatures that correspond to a two-step decrease of storage modulus. In contrast, for the membrane cast in DMAc, only one relaxation temperature is observed. For the $In0505_{DMSO}$, the first relaxation (at 220 °C) might correspond to motions of the chain of the hydrophobic domains,[36] while the second relaxation can be associated with the creeping of the whole chain, as due to the breaking of ionic interactions between the lithiated sulfonic side chains. It is interesting to point out that the relaxation temperature of the DMAc-cast membrane has a value between those of DMSO cast membranes. In addition, the relaxation peak is much larger. These findings suggest that the hydrophobic domains are well separated and percolated for the membrane cast from DMSO,

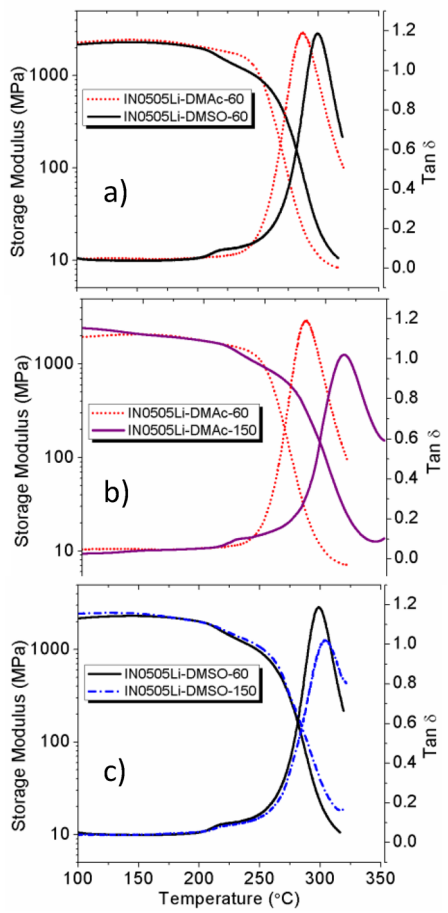

Figure 6. DMA profiles of In0505 membranes cast from both solvents: Storage modulus vs temperature and tan δ vs temperature. (a) Membranes cast from DMAc and DMSO solutions at 60 °C. (b) Membranes cast from DMAc at 60 °C and annealed at 150 °C (c) Membranes cast from DMSO at 60 °C and annealed at 150 °C (The membranes were washed in water and well dried before to perform DMA).

while the separation is much less effective in the case of the membrane cast from DMAc. The DMA results therefore corroborate the conclusions of the SANS study on the effect of solvent selection on the quality of phase separation.

With the aim to improve the membrane performances, the study was extended to a series of Inxx membranes of different block lengths obtained directly after the casting at 60 °C ("as-casting membrane"), and further annealed at 150 °C ("annealed membranes").

The thermo-mechanical behavior of annealed membranes was also investigated using DMA on the In0505 annealed membranes, and again, we find different behaviors in DMAc and DMSO membranes. A huge effect is noticed on the DMAc membranes (Figure 6b). A small peak appears on the tan δ plot, and the decrease of the storage modulus evolves toward two-slope behavior. As a consequence, the annealing process seems to significantly improve the phase separation between hydrophobic and hydrophilic chains. Interestingly, the annealed-DMAc membranes present similar thermo-mechanical responses as the nonannealed DMSO-cast membranes. This suggests that the annealing procedure transforms a rather poorly separated block material into a well-ordered block structure. Regarding the DMSO-cast membranes (Figure 6c),

DOI: 10.1021/acsami.5b01835
ACS Appl. Mater. Interfaces 2015, 7, 13808–13820

the annealing treatment has a very limited effect on the thermo-mechanical properties, with only a small shift of the main relaxation peak. As this peak is due to chain creeping because of the breaking of ionic bonds, the observed shift could be related to stronger interactions between ionic functions, which can be presumably related to a better local organization of ionic moieties within ionic domains.

3.4. Water Uptake and Conductivity. Following the study of In0505 and ps-FES morphology and thermo-mechanical properties, we explored the effects of solvent selectivity and annealing through the water uptake and conductivities.

3.4.1. "As-Casting Membranes". 3.4.1.1. Water Uptake. The capacity of the different membranes, i.e., ps-PES and Inxx, to uptake water was evaluated at different temperatures. The results expressed in λ (mol H_2O/mol SO_3^-H) are represented in Figure 7a and compared to Nafion 117 as a reference. We notice that the aromatic membranes exhibit higher water uptake as compared to Nafion 117.

From Figure 7a, significant effects of block structure, block length, and solvent selectivity on the water uptake of the ionomer membranes were observed. First, it is noteworthy to point out that despite having close IEC values with respect to block copolymer materials, the water uptake of the ps-PES based membrane drastically increases after 60 °C. Above 80 °C, it is completely soluble in water. In contrast, the membranes of block copolymers, Inxx, absorb a moderate amount of water and keep their integrity. This result clearly proves the advantage of block structure. However, with increasing block length of the Inxx, the water uptake increases significantly. Similar behavior was reported for the sulfonated multiblock copolymers and was explained by a better percolation of hydrophilic domains with increasing sulfonated block length.[27]

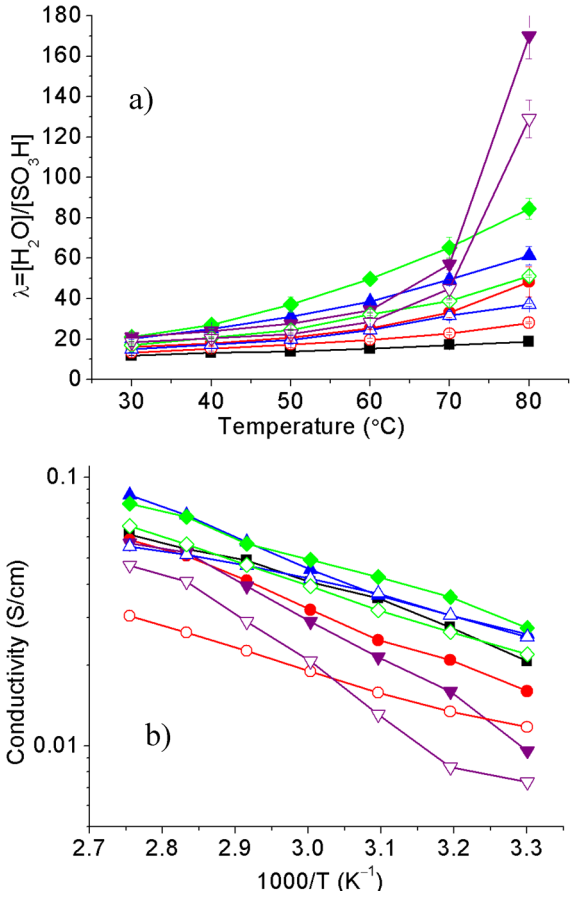

Figure 7. (a) Evolution of hydration number (λ) with the water immersing temperature (b) Evolution of proton conductivity with $1000/T$ at 95% RH for the following: Nafion 117 (black ■), $IN0505_{DMSO60}$ (red ●), $IN1010_{DMSO60}$(blue▲), $IN1515_{DMSO60}$ (green ◆), ps-PES_{DMSO60} (purple ▼), $IN0505_{DMAc60}$ (red ○), $IN1010_{DMAc60}$ (blue △), $IN1515_{DMAc60}$ (green ◇), and ps-PES_{DMAc60} (purple ▽). (Errors limits for conductivities are ±14%.)

A general finding is that the utilization of DMSO as a casting solvent increases the water uptake of resulting membranes as compared with those obtained from DMAc cast membranes. Such a difference seems to be more pronounced in the case of Inxx as compared to ps-PES. The reduced water uptake of films cast from DMAc could be explained by (i) the presence of isolated and less connected hydrophilic domains, as evidenced from the SANS analysis in the case of Inxx membranes and/or (ii) the amount of the residual casting solvent trapped in the membrane before its acidification. The latter hypothesis was checked by quantitatively analyzing the membrane composition by ^{1}H NMR after the drying process (on the membrane in lithium salt form). We observed that the amount of residual solvent, calculated from ^{1}H NMR (see Experimental Section), strongly depends on the solvent nature. In the case of DMSO cast membranes, about 10 wt % residual solvent was found while only 2 wt % in the case of DMAc cast membrane. At this stage, we can suppose that the solvent can be retained within the membranes by strong interactions with the lithium perfluorosulfonate, or trapped in hydrophobic or hydrophilic domains with high Tg (220 and 150 °C respectively[36]). In order to gain further insights, the membranes were also analyzed after their immersion in acidic water followed by washing with deionized water. Any presence of residual solvent was detected in the NMR spectra. Taking into account the high Tg of these polymers,[36] more specifically that of the hydrophobic block in Inxx materials (which cannot be plasticized by water molecules), we can hypothesize that (i) the residual solvent was mostly present in hydrophilic domains and therefore totally exchanged by water along the hydration process, yielding solvent free membranes at the end,(ii) more free volumes could be formed in the hydrophilic domains of dried membranes cast from DMSO as compared to those cast from DMAc due to the different amounts of residual solvent exchanged by the water. The presence of solvent-induced free volumes left after the casting process should affect the final gas permeability of the membranes. Therefore, we investigated the oxygen and hydrogen permeability properties in In0505 membranes prepared from DMSO and DMAc solutions and determined the respective permeation coefficients. The gas permeability of hydrophobic polymer, FPES membrane, was also measured. All data are summarized in Table 5. We observe that the copolymers In0505 exhibit similar oxygen permeability

Table 5. Gas Permeability Coefficients of the In0505 Copolymers Prepared from DMAc and DMSO Solvent and of the FPES Homopolymer

membrane	PH_2 (barrer)	PO_2 (barrer)
$In0505_{DMSO}$	7.83	0.48
$In0505_{DMAc}$	8.80	0.51
FPES	42.96	6.33

DOI: 10.1021/acsami.5b01835
ACS Appl. Mater. Interfaces 2015, 7, 13808−13820

coefficients independent of the casting solvent. Such a finding underlines that the difference in free volumes within the hydrophilic phase, as possibly due to higher residual solvent amount in DMSO-cast membranes, is not significant enough to play a predominant role in the gas transport mechanism in the anhydrous state. Moreover, the copolymer permeability coefficients are significantly lower than those measured on the FPES membrane. Such an important decrease of gas permeability, observed when ps-PES segments are bonded to FPES segments into In0505, supports the arrangement of sulfonated domains into a very low permeable phase under anhydrous conditions. This result is in agreement with similar trends already observed on sulfonated copolyimides.[60] Additionally, it is interesting to note that slightly higher hydrogen permeability values are obtained for $In0505_{DMAc60}$ in comparison to $In0505_{DMSO60}$. This effect could be assigned to a slightly higher extent of hydrophobic/hydrophilic interfacial regions in the first membrane. The permeation measurements hence nicely corroborate the morphological picture proposed after the SANS study, which evidenced the presence of isolated and less connected hydrophilic domains in DMAc-cast materials and the substantial increase of specific surface with respect to DMSO-cast membranes. According to the permeability results, these interfacial areas could contribute to gas diffusion only for molecules with small kinetic diameters.

To summarize these results, we conclude that the presence of variable quantities of residual solvents in the DMSO/DMAc cast membranes (before their acidification) do not have a substantial impact on gas permeability. Hence, the presence of limited/extended free volumes within the two types of membranes cannot primarily cause the observed water uptake variations. Accordingly, the water uptake behavior rather originates from the solvent-dependent morphologies induced by solvent-block specific interactions, as described in the SANS section. Increasing the degree of structural order (DMSO-cast materials) favors the incorporation of water molecules into the 3D interconnected network of regular ionic domains distributed within ordered blocky domains.

3.4.1.2. Conductivity. The effects of solvent selectivity as well as the block length of the multiblock copolymers were studied by measuring the proton conductivity (σ). Figure 7b presents the evolution of conductivities with $1000/T$, at 95% RH for membranes ps-PES and Inxx multiblock copolymers, prepared in both solvents (DMAc, DMSO) as well as Nafion 117 as reference for comparison. A general property regarding the impact of solvent selectivity on proton conductivities emerges from a direct inspection of Figure 6b. Indeed, it is seen that all membranes prepared from DMSO solution are more conductive than those obtained from DMAc. This situation could simply originate from the higher ability of DMSO-cast membranes to uptake water, as previously evidenced in Figure 7a. However, if we examine the results of Figure 7b more deeply, we can add several interesting comments on the effect of solvent selectivity. First, it can be underlined that the solvent selectivity seems to impact much more significantly In0505 as compared to ps-PES. We found a $\sigma_{DMSO/DMAc}$ ratio of almost 2 for In0505, while only a value of 1.3 for the ps-PES membranes. In addition, the proton conductivities of the multiblock copolymer membranes are shown to increase significantly with increasing block length, In1515 > In1010 > In0505. This effect is systematically observed for both DMSO and DMAc cast-membranes, but not to the same extent. Indeed, the $\sigma_{DMSO/DMAc}$ ratio diminishes when the block length increases, i.e., it decreases from 2 in the case of In0505 membranes to 1.5 and 1.4 for In1010 and In1515 membranes, respectively. Therefore, the shorter the blocks, the more the nature of the casting solvent impacts the overall membrane performance. We can tentatively ascribe such behavior to morphological peculiarities. Short blocks architectures could indeed be more sensitive to the introduction of structural disorder produced by the use of DMAc. In turn, on increasing the FPES segment size, the compatibilizing effect of DMAc is likely to be reduced; therefore more block-separated local units might possibly form.

It seems that increasing the block length does not lead to a proportional increase in proton conductivities. $In1010_{DMSO60}$ membranes conduct twice as well as $In0505_{DMSO}$ membranes, but only limited improvement is gained with $In1515_{DMSO60}$ membranes at low temperatures. At temperatures higher than 70 °C, the conductivities of DMAC-cast In1010 and In1515 are even comparable. This could indicate that there is an optimum for producing ordered-enough morphologies already reached with the 10 000 block size. We also note that the conductivities of ionomers In1010 and In1515 are close to those of Nafion 117 up to 60 °C, and higher at higher temperatures, showing the interesting potential of the as-cast block copolymer materials in view of fuel cell applications.

3.4.2. Annealed Membranes. The "as-cast membranes" in lithium salt form were annealed at 150 °C to probe the beneficial effect of thermal annealing on conductivities and water uptakes. The temperature of 150 °C was chosen in relation to the Tg of the "as-casting membrane" and the "annealed membrane". As can be seen from Figure 8 and Table

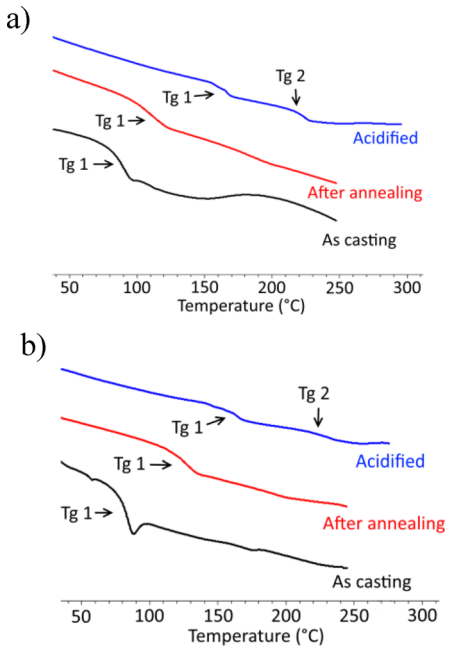

Figure 8. DSC diagrams of "as-cast" and "annealed" In1515 membranes cast from (a) DMAc and (b) DMSO.

6, the Tg of "as-casting membranes" ranges from 80 to 90 °C (Table 6) while after annealing, the Tg of the membranes increase by at least 20 °C, yet reaching maximum values around 110 °C. These values are much lower than those of ionomers in acidic or lithium form, as previously reported (Tg ionic domain ≈ 150 °C, Tg hydrophobic domains ≈ 220 °C).[36] This could be explained by the presence of residual solvent molecules

DOI: 10.1021/acsami.5b01835
ACS Appl. Mater. Interfaces 2015, 7, 13808−13820

Table 6. Thermal Transitions of As-Cast and Annealed Membranes

membrane	Tg (°C)	
	as-cast*	annealed**
$IN0505_{DMSO}$	88 ± 2	104 ± 2
$IN1010_{DMSO}$	78 ± 2	112 ± 2
$IN1515_{DMSO}$	80 ± 2	108 ± 2
$IN0505_{DMAc}$	83 ± 2	105 ± 2
$IN1010_{DMAc}$	78 ± 2	110 ± 2
$IN1515_{DMAc}$	82 ± 2	102 ± 2

which interact preferentially with ionic functions, leading to an important decrease of the Tg associated with the ionic domains. Thus, annealing under the present conditions (150 °C in the presence of residual solvent located predominately in ionic domains) is expected to favor the reorganization of ionic domains. After the thermal treatment, the amount of residual solvent in the annealed membrane, calculated by ^{1}H NMR analysis, decreases from 10 wt % to almost 8 wt % in the case of membranes cast from DMSO, and from 2% to almost 1% in the case of membrane cast from DMAc.

3.4.2.1. Conductivities and Water Uptakes. Thermal annealing of the copolymer membranes at 150 °C lead to lower water uptake and much improved conductivities as compared to those of membranes dried at 60 °C (Figure 9). For example, at 80 °C and 95% RH, the proton conductivity of $In0505_{DMSO150}$ is 2 times higher than that of $In0505_{DMSO60}$, and

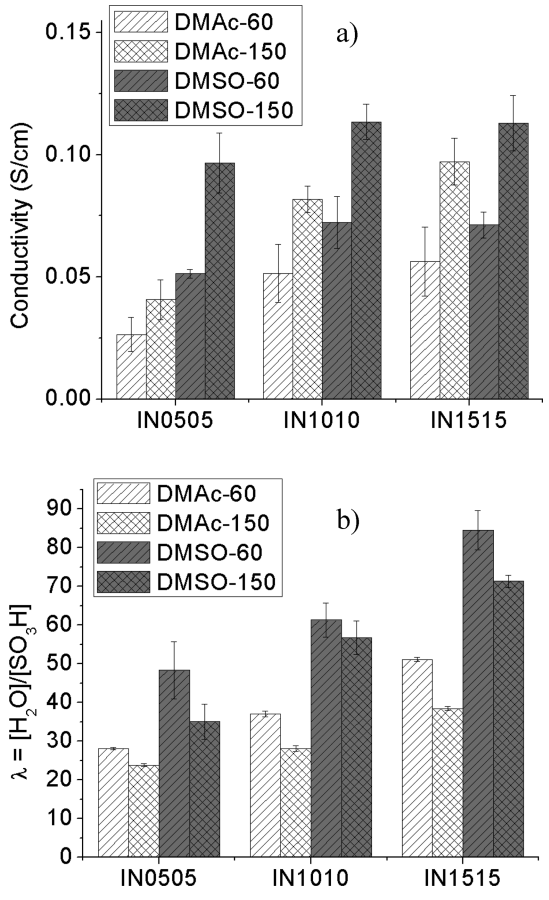

Figure 9. (a) Conductivities at 95% RH and (b) water uptake (the hydration number) at 80 °C of annealed and nonannealed membranes.

1.3 higher than Nafion 117, while the water uptake is decreased by 20%. All the membranes (except $In0505_{DMAc150}$) show higher conductivities than Nafion 117 in the investigated range of temperatures (Figure 10). This spectacular increase of

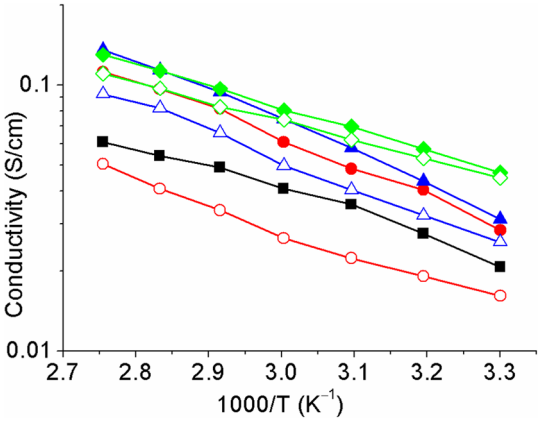

Figure 10. Evolution of proton conductivity with $1000/T$ at 95% of RH of INxx annealed membranes: $IN0505_{DMSO150}$ (red ●), $IN1010_{DMSO150}$ (blue ▲), $IN1515_{DMSO150}$ (green ◆), $IN0505_{DMAc150}$ (red ○), $IN1010_{DMAc150}$ (blue △), $IN1515_{DMAc150}$ (green ◇), Nafion 117 (black ■). (Errors limits for conductivities are ±14%.)

conductivities is observed for the membranes cast from both solvents, with a gain almost of the same order of magnitude with respect to nonannealed materials. The striking difference in the conducting behavior between annealed and nonannealed samples, along with the greatly reduced water uptake upon annealing, suggests that the annealing treatment permits a more efficient proton transport within the phase-separated material. This could be due to a beneficial impact of annealing on the cocontinuous nanophase separated morphology, the local arrangement of neighboring side chains and/or improved connectivity of ionic channels, and favorable organization of conductive domains at higher scales. The hypothesis of structural reorganization is supported by our DMA analysis.

Regarding the impact of casting solvent selectivity on the membrane conductivities, it is interesting to point out that the gaps in conductivity of Inxx membranes cast in DMSO and DMAc remain on the same order of magnitude as those of membranes cast at 60 °C. The $\sigma_{DMSO/DMAc}$ ratio is about 2 in annealed In0505, whereas for In1010 and In1515, we found values of 1.3 and 1.2, respectively (Figure 9). Accordingly, the local topology of ionic domains as well as the ionic network connectivity must be substantially improved by the thermal treatment for membranes obtained from both solvents. As the annealing temperature is lower than the Tg of the hydrophobic blocks, it can be hypothesized that the thermal treatment mostly induce reorganization of ionic domains due to pendant chain relaxations and enhanced mobility.

The impact of RH on proton conductivity has been studied for these multiblock copolymers membranes cast from DMSO. Figure 11 shows the proton conductivity at 80 °C as a function of RH for annealed and nonannealed membranes. Again, it is not surprising to observe the huge impact of annealing on the conductivity, especially at low RH. At 30% RH, the conductivities of annealed membranes are 10 times higher than those of nonannealed ones. Moreover, we obtain conductivity values for $In1515_{DMSO150}$ similar to those of Nafion 117. Another important result is the lower dependence

DOI: 10.1021/acsami.5b01835
ACS Appl. Mater. Interfaces 2015, 7, 13808−13820

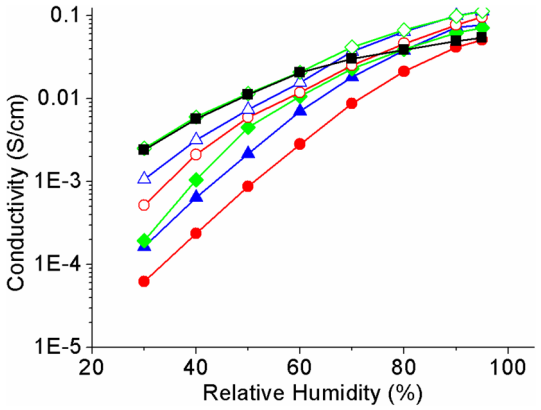

Figure 11. Proton conductivity at 80 °C: Nafion 117 (black ■), $IN0505_{DMSO60}$ (red ●), $IN1010_{DMSO60}$(blue ▲), $IN1515_{DMSO60}$(green ◆), $IN0505_{DMSO150}$ (red ○), $IN1010_{DMSO150}$ (blue △), $IN1515_{DMSO150}$(green ◇). (Errors limits for conductivities are ±14%.)

of the proton conductivity of the annealed membrane on the humidity levels. Combined with the aforesaid beneficial effects of annealing in reducing water uptake and improving phase separation between the hydrophilic and hydrophobic domains, this observation further confirms the importance of membrane elaboration in developing PEM with excellent performances.

4. CONCLUSIONS

The overall goal of the present work was to study how the solvent selectivity, block length, and thermal annealing affect the functional properties (conductivity and water uptake) of new promising ionomers, i.e., Perfluorosulfonated Poly(arylene ether sulfone) Multiblock Copolymers. To determine the degree of selectivity of the solvent, the Flory−Hugins parameters between selected solvents and ps-PES and FPES blocks, respectively, were calculated by an original method, i.e., IGC. DMSO and DMAc were selected as casting solvents for the study, as DMSO was identified to be a selective solvent, while DMAc is able to dissolve both segments of the copolymers. The selectivity of the solvents was shown to have no significant impact on the expansion of ionic domains upon swelling, while it dramatically affects the supramolecular ordering of the blocks. This finding highlights the complex interplay between solvent-modulated local interactions, peculiar block-induced morphologies, and hydration-dependent hydrophilic domains topology. We show that PEM performance is determined by a subtle balance between these effects, which was noticeably optimized by thermal treatment.

The combination of block length-casting solvent selectivity-membrane processing conditions was shown to result in a very significant increase in performance, with conductivities higher than state-of-the art PFSA membranes.

This study provides a detailed understanding of how block copolymer properties are affected by block length averages and the elaboration method, providing essential clues for a more rational design of efficient block copolymer membranes for fuel cells.

■ ASSOCIATED CONTENT

Ⓢ Supporting Information

A short description on calculation of the Flory−Huggins parameters are presented. The Supporting Information is available free of charge on the ACS Publications website at DOI: 10.1021/acsami.5b01835.

■ AUTHOR INFORMATION

Corresponding Author

*Phone: +33 (0)476 82 65 61. Fax: +33 (0)476 82 67 77. E-mail: Cristina.Iojoiu@lepmi.grenoble-inp.fr (C.I.).

Author Contributions

The manuscript was written through contributions of all authors.

Notes

The authors declare no competing financial interest.

■ ACKNOWLEDGMENTS

The authors would like to thank the FEDER-FUI France for providing financial support to this research work in the framework of the project "Nano-structurated High Performance Polymer". The Institut Laue Langevin is acknowledged for providing access to beam time, and we are grateful to L. Porcar for beamline alignment and his kind help during the experiments. We thank S. Papadopoulou for his help with the ICG column preparation. This work was performed within the framework of the Centre of Excellence of Multifunctional Architectured Materials "CEMAM" no. AN-10-LABX-44−01.

■ REFERENCES

(1) Zhang, H.; Shen, P. K. Advances in the High Performance Polymer Electrolyte Membranes for Fuel Cells. *Chem. Soc. Rev.* **2012**, *41*, 2382−2394.
(2) Mauritz, K. A.; Moore, R. B. State of Understanding of Nafion. *Chem. Rev.* **2004**, *104*, 4535−4585.
(3) Paddison, S. J.; Paul, R. The Nature of Proton Transport in Fully Hydrated Nafion. *Phys. Chem. Chem. Phys.* **2002**, *4*, 1158−1163.
(4) Peron, J.; Mani, A.; Zhao, X.; Edwards, D.; Adachi, M.; Soboleva, T.; Shi, Z.; Xie, Z.; Navessin, T.; Holdcroft, S. Properties of Nafion NR-211 membranes for PEMFCs. *J. Membr. Sci.* **2010**, *356*, 44−51.
(5) Haubold, H.-G.; Vad, T.; Jungbluth, H.; Hiller, P. Nanostructure of Nafion: A SAXS study. *Electrochim. Acta* **2001**, *46*, 1559−1563.
(6) Duan, Q.; Wang, H.; Benziger, J. Transport of Liquid Water Through Nafion Membranes. *J. Membr. Sci.* **2012**, *392*−*393*, 88−94.
(7) Kerres, J. A. Development of Ionomer Membranes for Fuel Cells. *J. Membr. Sci.* **2001**, *185*, 3−27.
(8) Hickner, M. A.; Ghassemi, H.; Kim, Y. S.; Einsla, B. R.; McGrath, J. E. Alternative Polymer Systems for Proton Exchange Membranes (PEMs). *Chem. Rev.* **2004**, *104*, 4587−4612.
(9) Kreuer, K.-D. Ion Conducting Membranes for Fuel Cells and other Electrochemical Devices. *Chem. Mater.* **2014**, *26*, 361−380.
(10) Collette, F. M.; Lorentz, C.; Gebel, G.; Thominette, F. Hygrothermal Aging of Nafion. *J. Membr. Sci.* **2009**, *330*, 21−29.
(11) Rozière, J.; Jones, D. J. Non-Fluorinated Polymer Materials for Proton Exchange Membrane Fuel Cells. *Annu. Rev. Mater. Res.* **2003**, *33*, 503−555.
(12) Choi, J.-H.; Ye, Y.; Elabd, Y. A.; Winey, K. I. Network Structure and Strong Microphase Separation for High Ion Conductivity in Polymerized Ionic Liquid Block Copolymers. *Macromolecules* **2013**, *46*, 5290−5300.
(13) Hoarfrost, M. L.; Segalman, R. A. Ionic Conductivity of Nanostructured Block Copolymer. *Macromolecules* **2011**, *44*, 5281−5288.
(14) Young, W.-S.; Epps, T. H. Ionic Conductivities of Block Copolymer Electrolytes, with various Conducting Pathways: Sample Preparation and Processing Considerations. *Macromolecules* **2012**, *45*, 4689−4697.
(15) Weber, R. L.; Ye, Y.; Schmitt, A. L.; Banik, S. M.; Elabd, Y. A.; Mahanthappa, M. K. Effect of Nanoscale Morphology on the

Conductivity of Polymerized Ionic Liquid Block Copolymers. *Macromolecules* **2011**, *44*, 5727−5735.
(16) Virgili, J. M.; Hoarfrost, M. L.; Segalman, R. A. Effect of an Ionic Liquid Solvent on the Phase Behavior of Block Copolymers. *Macromolecules* **2010**, *43*, 5417−5423.
(17) Torquato, S. Optimal Design of Heterogeneus Materials. *Annu. Rev. Mater. Res.* **2010**, *40*, 101−129.
(18) Bates, F. S.; Fredricjson, G. H. Block Copolymers—Designer Soft Materials. *Phys. Today* **1999**, *52*, 32−38.
(19) Lee, H. S.; Roy, A.; Lane, O.; Dunn, S.; McGrath, J. E. Hydrophilic−hydrophobic Multiblock Copolymers Based on Poly(arylene ether sulfone) via Low-Temperature Coupling Reactions for Proton Exchange Membrane Fuel Cells. *Polymer* **2008**, *49*, 715−723.
(20) Lee, H. S.; Roy, A.; Lane, O.; McGrath, J. E. Synthesis and Characterization of Poly(arylene ether sulfone)-*b*-Polybenzimidazole Copolymers for High Temperature Low Humidity Proton Exchange Membrane Fuel Cells. *Polymer* **2008**, *49*, 5387−5396.
(21) Lee, H. S.; Badami, A.; Roy, A.; McGrath, J. E. Segmented Sulfonated Poly(Arylene Ether Sulfone)-*b*-Polyimide Copolymers for Proton Exchange Membrane Fuel Cells. Copolymer Synthesis and Fundamental Properties. *J. Polym. Sci., Part A: Polym. Chem.* **2007**, *45*, 4879−4890.
(22) Zhao, C.; Lin, H.; Shao, K.; Le, X.; Ni, H.; Wang, Z.; Na, H. Block Sulfonated Poly(ether ether ketone)s (SPEEK) Ionomers with High Ion-Exchange Capacities for Proton Exchange Membranes. *J. Power Sources* **2006**, *162*, 1003−1009.
(23) Wang, H.; Badami, A.; Roy, A.; McGrath, J. E. Multiblock Copolymers of Poly(2,5-benzophenone) and Disulfonated Poly(arylene ether sulfone) for Proton-Exchange Membranes. I. Synthesis and Characterization. *J. Polym. Sci., Part A: Polym. Chem.* **2007**, *45*, 284−294.
(24) Lee, M.; Park, J. K.; Lee, H.-S.; Lane, O.; Moore, R. B.; McGrath, J. E.; Baird, D. G. Effects of Block Length and Solution-Casting Conditions on the Final Morphology and Properties of Disulfonated Poly(arylene ether sulfone) Multiblock Copolymer Films for Proton Exchange Membranes. *Polymer* **2009**, *50*, 6129−6138.
(25) Assumma, L.; Iojoiu, C.; Albayrakari, G.; Cointeaux, L.; Sanchez, J.-Y. Polysulfone Containing Sulfonamide Groups as Proton Exchange Membrane for Fuel Cells. *Int. J. Hydrogen Energy* **2014**, *39*, 2740−2750.
(26) Cho, C. G.; Kim, Y. S.; Yu, X.; Hill, M.; McGrath, J. E. Synthesis and Characterization of Poly(arylene ether sulfone) Copolymers with Sulfonimide Side Groups for a Proton-Exchange Membrane. *J. Polym. Sci, Part A: Polym. Chem.* **2006**, *44*, 6007−6014.
(27) Yoshimura, K.; Iwasaki, K. Aromatic Polymer with Pendant Perfluoro Alkyl Sulfonic Acid for Fuel Cell Applications. *Macromolecules* **2009**, *42*, 9302−9306.
(28) Li, H.; Jackson, A. B.; Kirk, N. J.; Mauritz, K. A.; Storey, R. F. Poly(arylene ether sulfone), Statistical Copolymers Bearing Perfluoroalkylsulfonic Acid Moieties. *Macromolecules* **2011**, *44*, 694−702.
(29) Nakabayashi, K.; Higashihara, T.; Ueda, M. Polymer Electrolyte Membranes Based on Poly(Phenylene ether)s with Pendant Perfluoro Alkyl Sulfonic Acids. *Macromolecules* **2011**, *44*, 1603−1609.
(30) Xu, K.; Oh, H.; Hickner, M. A.; Wang, Q. Highly Conductive Aromatic Ionomers with Perfluorosulfonic Acid Side Chains for Elevated Temperature Fuel Cells. *Macromolecules* **2011**, *44*, 4605−4609.
(31) Miyatake, K.; Shimura, T.; Mikami, T.; Watanabe, M. Aromatic Ionomers with Superacids Groups. *Chem. Commun.* **2009**, *42*, 6403−6405.
(32) Mikami, T.; Miyatake, K.; Watanabe, M. Poly(arylene ether)s Containing Super Acid Groups as Proton Exchange Membranes. *ACS Appl. Mater. Interfaces* **2010**, *2*, 1714−1721.
(33) Chang, Y.; Brunello, G. F.; Fuller, J.; Disabb-Miller, M. L.; Hawley, M. E.; Kim, Y. S.; Hickner, M. A.; Jang, S. S.; Bae, C. Polymer Electrolyte Membranes Based on Poly(arylene ether sulfone) with Pendant Perfluorosulfonic Acid. *Polym. Chem.* **2013**, *4*, 272−281.
(34) Chang, Y.; Brunello, G. F.; Fuller, J.; Hawley, M.; Kim, Y. S.; Disabb-Miller, M.; Hickner, M. A.; Jang, S. S.; Bae, C. Aromatic Ionomers with Highly Acidic Sulfonate Groups: Acidity, Hydration, and Proton Conductivity. *Macromolecules* **2011**, *44*, 8458−8469.
(35) Mikami, T.; Miyatake, K.; Watanabe, M. Synthesis and Properties of Multiblock Copoly(arylene ether)s Containing Superacid Groups for Fuel Cell Membranes. *J. Polym. Sci., Part A: Polym. Chem.* **2011**, *49*, 452−464.
(36) Assumma, L.; Nguyen, H. D.; Iojoiu, C.; Lyonnard, S.; Mercier, R.; Planes E. Synthesis of Partially Fluorinated Poly(arylene ether sulfone) Multiblock Copolymers Bearing Perfluorosulfonic Functions. *J. Polym. Sci. A: Polym. Chem.* on line DOI 10.1002/pola27650.
(37) Assumma, L.; Iojoiu, C.; Mercier, R.; Lyonnard, S. Structure-Transport Interplay in New Aromatic Block Ionomers, *Macromolecules* under submission.
(38) Park, C. H.; Lee, C. H.; Guiver, M. D.; Lee, Y. M. Sulfonated Hydrocarbon Membranes for Medium-Temperature and Low-Humidity Proton Exchange Membrane Fuel Cells (PEMFCs). *Prog. Polym. Sci.* **2011**, *36*, 1443−1498.
(39) Robertson, G. P.; Mikhailenko, S. D.; Wang, K.; Xing, P.; Guiver, M. D.; Kaliaguine, S. Casting Solvent Interactions with Sulfonated Poly(ether ether ketone) During Proton Exchange Membrane Fabrication. *J. Membr. Sci.* **2003**, *219*, 113−121.
(40) Noda, A.; Susan, M. A. B. H.; Kudo, K.; Mitsushima, S.; Hayamizu, K.; Watanabe, M. Brønsted Acid−Base Ionic Liquids as Proton Conducting Nonacqueus Electrolyte. *J. Phys. Chem. B* **2003**, *107*, 4024−4033.
(41) Hamley, I. W. *Introduction to Block Copolymers, Developments in Block Copolymer Science and Technology*; John Wiley & Sons, Ltd: New York, 2004, Vol. *1*, pp 1−29.
(42) Adams, F. V.; Nxumalo, E. N.; Krause, R. W. M.; Hoek, E. M. V; Mamba, B. B. The Influence of Solvent Properties on the Performances of Polysulfone/*β*-Cyclodextrin Polyurethane Mixed Matrix Membranes. *J. Appl. Polym. Sci.* **2013**, *130*, 2005−2014.
(43) Mineart, K. P.; Jiang, X.; Jinnai, H.; Takahara, A.; Spontak, R. J. Morphological Investigation of MidBlock Sulfonated Block Ionomers Prepared from Solvents Differing in Polarity. *Macromol. Rapid Commun.* **2015**, *36* (5), 432−438.
(44) Zhang, F.; Zhang, H.; Qu, C. Influence of Solvent on Polymer Prequaternization toward Anion-Conductive Membrane Fabrication for All-Vanadium Flow Battery. *J. Phys. Chem. B* **2012**, *116*, 9016−9022.
(45) Li, W.; Zhang, F.; Yi, S.; Huang, C.; Zhang, H.; Pan, M. Effects of Casting Solvent on Microstructrue and Ionic Conductivity of Anhydrous Sulfonated Poly(ether ether ketone)-inoic Liquid Composite Membranes. *Int. J. Hydrogen Energy* **2012**, *37*, 748−754.
(46) Jun, M.-S.; Choi, Y.-W.; Kim, J.-D. Solvent Casting Effects of Sulfonated Poly(ether ether ketone) for Polymer Electrolyte Membrane Fuel Cell. *J. Membr. Sci.* **2012**, *396*, 32−37.
(47) Cho, K.-Y.; Park, J.-K.; Jung, H.-Y. The Effect of Solvent Casting Condition on the Electrochemical Properties of Nafion/Polyvinylidene Fluoride Copolymer Blends for Direct Methanol Fuel Cell. *Chem. Eng. Commun.* **2015**, *202*, 593−599.
(48) Ding, X.; Didari, S.; Fuller, T. F.; Harris, T. A. L. Effects of Annealing Conditions on the Performances of Solution Cast Nafion Membranes in Fuel Cells. *J. Electrochem. Soc.* **2013**, *160*, F793−F797.
(49) Alberti, G.; Narducci, R.; Di Vona, M. L.; Giancola, S. Annealing of Nafion 1100 in the Presence of an Annealing Agent: A Powerful Method for Increasing Ionomer Working Temperature in PEMFCs. *Fuel Cells* **2013**, *13*, 42−47.
(50) Wang, J.; Yang, M.; Dou, P.; Wang, X.; Zhang, H. Influences of Annealing on the Perfluorosulfonated Ion-Exchange Membranes Prepared by Melt Extrusion. *Ind. Eng. Chem. Res.* **2014**, *53*, 14175−14182.
(51) Yang, L.; Tang, J.; Li, L.; Ai, F.; Chen, X.; Yuan, W. Z.; Zhang, Y. Properties of Precursor Solution Cast PFSI Membranes with Various Ion Exchange Capacities and Annealing Temperatures. *RSC Adv.* **2013**, *3*, 7289−7295.
(52) Conder, J. R.; Young, C. L. *Physicochemical Measurement by Gas Chromatography*; Wiley: New York, 1979.

DOI: 10.1021/acsami.5b01835
ACS Appl. Mater. Interfaces 2015, 7, 13808−13820

(53) Al-Saigh, Z. Y.; Munk, P. Study of Polymer−Polymer Interaction Coefficients in Polymer Blends Using Inverse Gas-Chromatography. *Macromolecules (Washington, DC, U. S.)* **1984**, *17*, 803−809.
(54) Papadopoulou, S. K.; Dritsas, G.; Karapanagiotis, I.; Zuburtikudis, I.; Panayiotou, C. Surface Characterization of Poly-(2,2,3,3,3-pentafluoropropyl methacrylate) by Inverse gas Chromatography and Contact Angle Measurements. *Eur. Polym. J.* **2010**, *46*, 202−208.
(55) Papadopoulou, S. K.; Panayiotou, C. Thermodynamic Characterization of Poly(1,1,1,3,3,3-hexafluoroisopropyl methacrylate) by Inverse Gas Chromatography. *J. Chromatogr. A* **2012**, *1229*, 230−236.
(56) Naik, H. G.; Aminabhavinaik, T. M. Gas−Liquid Chromatographic Study of Polystyrene−*n*-Alkane Interactions. *J. Appl. Polym. Sci.* **2001**, *80*, 1291−1298.
(57) Kreuer, K. D.; Portale, G. A. A Critical Revision of the Nano-Morphology of Proton Conducting Ionomers and Polyelectrolytes for Fuel Cell Applications. *Adv. Funct. Mater.* **2013**, *23*, 5390−5397.
(58) Litt, M. H. A Reevaluation of Nafion Morphology. *Polym. Prepr.* **1997**, *38*, 80−81.
(59) Rubatat, L.; Gebel, G.; Diat, O. Evidence of Elongated Polymer Aggregates in Nafion. *Macromolecules* **2004**, *37*, 7772−7783.
(60) Piroux, F.; Espuche, E.; Mercier, R.; Pinéri, M.; Gebel, G. Gas Transport Mechanism in Sulfonated Polyimides Consequences on Gas Selectivity. *J. Membr. Sci.* **2002**, *209*, 241−253.

DOI: 10.1021/acsami.5b01835
ACS Appl. Mater. Interfaces 2015, 7, 13808−13820